LA-UR -86-420
CONF-8510273--2

Los Alamos National Laboratory is operated by the University of California for the United States Department of Energy under contract W-7405-ENG-36.

TITLE: COMPUTER SIMULATION OF MICROSTRUCTURAL DYNAMICS

LA-UR--86-420

DE86 006045

AUTHOR(S): G. S. Grest
M. P. Anderson
D. J. Srolovitz

SUBMITTED TO: The proceedings of the "Computer Simulation of Microstructural Evolution, Symposium," held in Toronto, Canada, October 14-17, 1985.

DISCLAIMER

Los Alamos Los Alamos National Laboratory
Los Alamos, New Mexico 87545

COMPUTER SIMULATION OF MICROSTRUCTURAL DYNAMICS

G. S. Grest*, M. P. Anderson* and D. J. Srolovitz**

*Corporate Research Science Laboratory
Exxon Research and Engineering Company
Annandale, New Jersey 08801

**Los Alamos National Laboratory
Los Alamos, New Mexico 87545

Abstract

Since many of the physical properties of materials are determined by their microstructure, it is important to be able to predict and control microstructural development. A number of approaches have been taken to study this problem, but they assume that the grains can be described as spherical or hexagonal and that growth occurs in an average environment. We have developed a new technique to bridge the gap between the atomistic interactions and the macroscopic scale by discretizing the continuum system such that the microstructure retains its topological connectedness, yet is amenable to computer simulations. Using this technique we have studied grain growth in polycrystalline aggregates. The temporal evolution and grain morphology of our model are in excellent agreement with experimental results for metals and ceramics.

Introduction

The physical and chemical properties of materials are determined, in part, by their microstructure. Both grain size and texture affect yield strength, fracture, surface adsorption phenomena and other properties. The final grain morphology can be modified by thermal processing, addition of a second phase, deformation, etc. However, in order to effectively tailor the microstructure for specific applications, the mechanism and kinetics of grain growth and recrystallization must be understood. Unfortunately, present theories (1-5) predict grain growth kinetics which differ from experimental observations, have little ability to predict microstructural details and cannot be readily generalized to account for the variety of experimentally controllable features.

Historically, a number of different theoretical approaches have been taken to understand and predict the microstructures of polycrystalline materials. These include analytical theory (1-5), finite element analysis (6), molecular dynamics simulations (7) and physical-analogue models [e.g. bubble rafts] (8), hard sphere models (9) and photoelastic models (10). Whereas analytical models have the virtue of producing closed form solutions, they are usually too oversimplified to quantitatively describe real physical systems. Even when numerical solutions of these analytical theories are performed, this difficulty persists. In principle, molecular dynamics is an ideal way to consistently incorporate the known forces and kinetic processes involved in microstructural evolution. However, present day computer memory and speed limits the technique to small clusters of atoms ($\lesssim 10^5$), which are typically too small to effectively represent more than a single microstructural feature. Whereas physical-analogue models lead to some insight, they are usually crude analogues to the actual physical process.

Since one of the essential features of grain growth or recrystallization in polycrystalline materials involves the competition between individual grains, of different orientations which share a common boundary, it is not surprising that existing grain growth theories have done so poorly in describing more than simple qualitative aspects of the experimentally observed kinetics and topology. Most analytic theories (1,3,4) implicitly assume that grains can be described as spherical, and that growth occurs in an average environment. This type of theory leads immediately to the result that the average grain radius

$$\bar{R} = B\, t^n \qquad (1)$$

where B is a temperature dependent constant and $n = 1/2$. This is in contrast to experimental data for n which, while showing substantial scatter, consistently give $n < 1/2$, with a mean value of approximately 0.4 (11). In addition, these macroscopic theories, incorrectly predict the grain size distribution function and make no prediction at all for many topological quantities, like the distribution of the number of grain edges. These failures and inabilities may be traced to their treating grain growth in terms of a grain in a mean environment. This type of mean field theory averages out much of the important, topological effects associated with connectedness of the actual microstructure. Generalizations of this type of theory (12-13) to include many interacting spherical grains, are also not sufficient as they still do not include the simple space-filling requirements which result in a topologically connected structure.

The present outlook for finding a solution of an analytical model for grain growth, which can correctly predict the topological features, does

not seem hopeful. In addition, it is also not possible at this time to carry out a realistic atomistic simulation using molecular dynamics to study grain growth or recrystallization. The computer resources for simulating a system of even 10^6 atoms is several years away. Thus, a method to bridge this gap between the atomistic and macroscopic scale is necessary. One method which we (14-17) have pursued is to discretize continuum models for microstructural evolution such that they are amenable to large scale computer simulations. The essential elements of this approach (which will be described in more detail below) consist of mapping the continuum microstructure onto a discrete lattice and defining interactions and dynamics for individual, discrete elements which are analogous to those in continuous systems.

There are several advantages to this type of procedure. The first is that one can incorporate at the most basic level different, often competing, driving forces. This is done by defining the energetics, and hence forces, for each individual element. These energetics include both interactions with surrounding elements and external stimuli. The second advantage is that, not only are complex microstructures generated from simple postulates, but that one can observe the temporal evolution of the microstructures, as well as the micro-mechanisms which lead to its development. In addition, microstructures may be generated which are consistent with any set of postulates as to the nature of the local dynamics and energetics. In this way, the testing of theoretical hypotheses can be performed by comparing simulated microstructures against those experimentally observed, similar to structure determination in x-ray diffraction (18) and lattice imaging (19) in electron microscopy. Finally, in terms of computer resources, both the memory and CPU time requirements are readily available on today's main frame computers.

In this paper we will describe, in more detail, the mapping onto a discrete lattice and the Monte Carlo alogarithm used in the simulations. As an example of how the method works, we will review our work on grain growth. In a companion paper (20) in these Proceedings, we will describe our work on abnormal grain growth and recrystallization. Finally, we will review several possible applications of the methodology to other problems.

The Model and Monte Carlo Method

In order to incorporate the complexity of grain boundary topology, the microstructure is mapped onto a discrete lattice (Fig. 1). Each lattice site is assigned a number between 1 and Q corresponding to the orientation of the grain in which it is embedded. We choose Q large enough so that grains of like orientation impinge infrequently, typically Q = 48 or 64. Since the speed of the computer alogarithm decreases with increasing Q, larger values of Q are not routinely employed. However, for $Q \gtrsim 36$, our results are insensitive to the magnitude of Q. In the present model, a grain boundary segment is defined to lie between two sites of unlike orientation. The grain boundary energy is specified by defining an interaction between lattice sites within a given distance [usually nearest neighbor in two-dimensions (2-d) and up to the third nearest neighbors in three-dimensions (3-d)],

$$E_i = -J \sum_j (\delta_{S_i S_j} - 1). \qquad (2)$$

Here S_i is the orientation of site i ($1 \leq S_i \leq Q$), δ_{AB} is the Kronecker delta and the sum is taken over all sites within a specified distance.

The kinetics of boundary motion are simulated via a Monte Carlo technique in which a site is selected at random and re-oriented to a

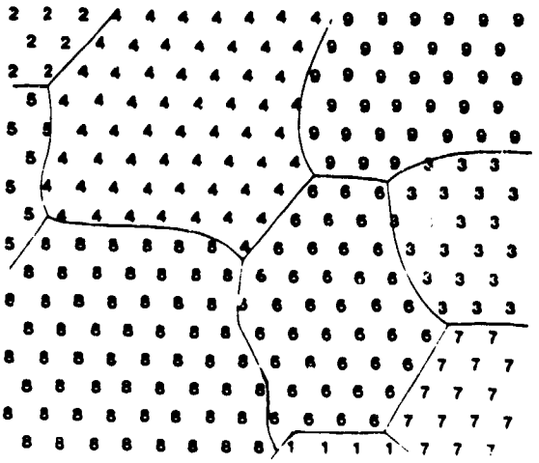

Figure 1 - Sample microstructure mapped onto a triangular lattice. The integers denote orientations and the lines represent grain boundaries.

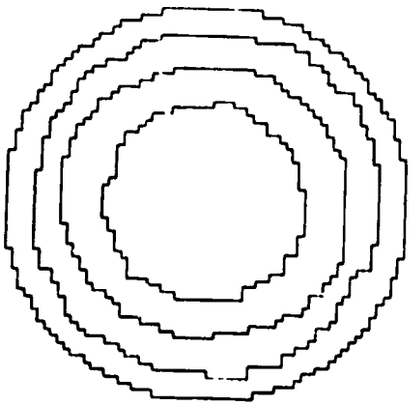

Figure 2 - Evolution of an initially spherical grain of initial radius R_o = 30 (in units of lattice sites) in an infinite matrix on a simple cubic lattice for t = 0, 200, 400 and 600 MCS.

randomly chosen orientation between 1 and Q. If the change in energy associated with the re-orientation, ΔE, is less than or equal to zero the re-orientation is accepted. However, if the re-orientation attempt results in $\Delta E > 0$, the re-orientation is accepted with probability $\exp(-\Delta E/k_BT)$, where k_BT is the thermal energy. A modified version of this alogorithm has been employed to make the simulation more efficient (see Ref. 17). A unit segment of grain boundary, therefore, moves with a velocity, $v_i = C[1-\exp(-\Delta E_i/k_BT)]$, where C is a constant proportional to the boundary mobility. This description of the local boundary velocity is formally equivalent to that derived from classical reaction rate theory. Time, in these simulations, is proportional to the number of re-orientation attempts. N re-orientation attempts is used as the unit of time and is referred to as 1 Monte Carlo Step (MCS), where N is the number of lattice sites. The conversion from MCS to real time has an implicit activation energy factor, $\exp(-W/k_BT)$, which corresponds to the atomic jump frequency. Since the quoted times are normalized by the jump frequency, the only effect of choosing T ≠ 0 (as in these simulations) is to restrict the accepted re-orientation attempts to those with $\Delta E \leq 0$. Re-orientation of a site at a grain boundary corresponds to boundary migration.

Results

We have carried out extensive simulations in both 2-d and 3-d. Most of our studies in 2-d have been on a triangular lattice of size 200^2, though we have also carried out simulations on the square and honeycomb lattice. Our results for 3-d are for the simple cubic lattice of size 60^3 and 100^3. One remarkable conclusion from our study is that most of the results are independent of dimensionality (for $d \geq 2$). For example, the grain area distribution and topological distribution of the number of edges is the same for the growth in the plane and for the cross-section of the 3-d microstructures. This result allows us to carry out many simulations in two-dimensions, where it is possible to study systems with much larger linear dimensions than in 3-d.

As a test of the simulation procedure, it is useful to examine the

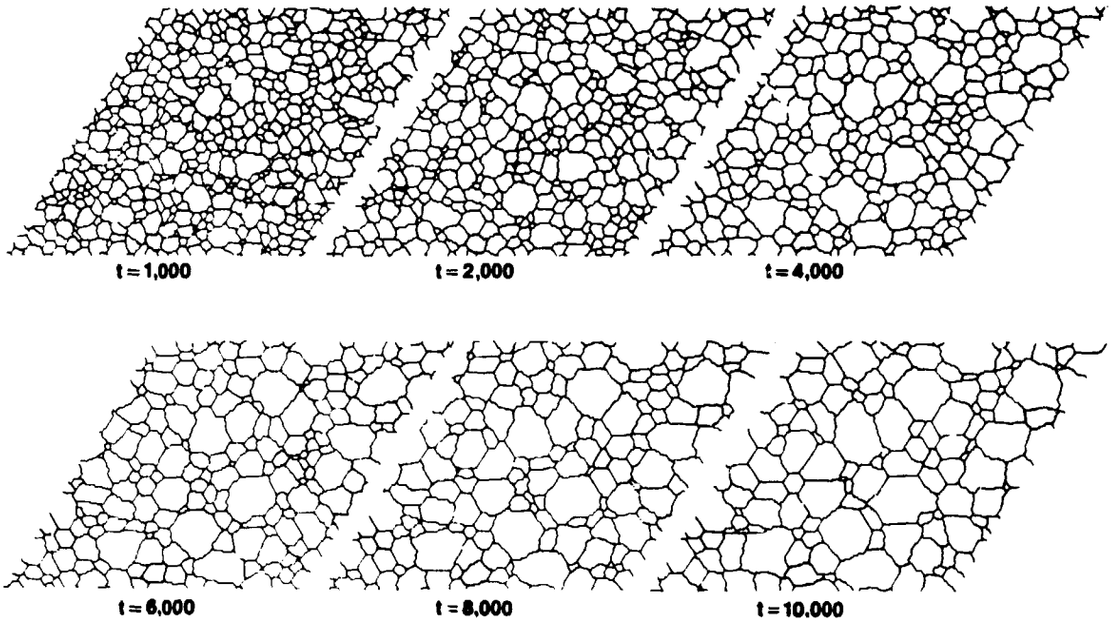

Figure 3 - Temporal evolution of a two-dimensional polycrystalline microstructure on a 200^2 triangular lattice for a pure, isotropic material. Grains with six edges have been shaded.

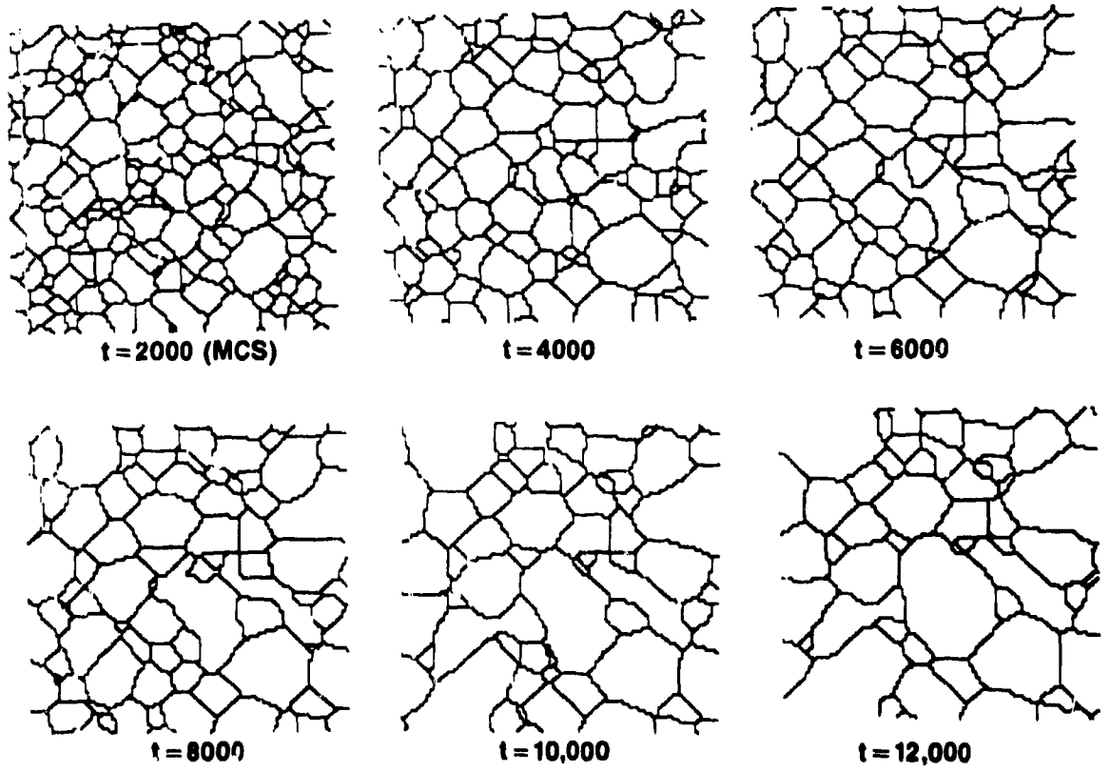

Figure 4 - Temporal evolution of the cross-section from the 3-d microstructure for Q = 48 on a 100^3 simple cubic lattice.

matrix (21). This is the case where the analytical theory applies. In Fig. 2 we show one of the great circles of a shrinking sphere at four different times. Similar results are obtained for a shrinking circle in 2-d. We observe that the radius decreases as the square of time, n = 1/2 in Eq. (1). This shows that the kinetic simulation technique employed is in agreement with the rate theory model of boundary motion.

For the simulations of polycrystalline grain growth, the microstructure is initialized by randomly assigning an orientation between 1 and Q to each lattice site. The temporal evolution of a polycrystalline microstructure is shown in Fig. 3 for growth on a 2-d triangular lattic and in Fig. 4 for a (100) planar section on the 3-d simple cubic lattice with first, second and third nearest neighbor interactions. Steps are clearly visible in the micrographs in Fig. 4 due to the small size of the simulated volume (100^3 lattice sites) though this is less visible in Fig. 3 for a 200^2 system. From these figures, it appears that the grain size distribution is nearly identical between 2-d and 3-d. This correspondence is made more quantitative in Fig. 5, where the grain radius distribution function is shown for the 2-d and 3-d samples. These distributions were found to be time invariant when normalized by their respective means. This property, which Mullins (22) refers to as statistical self-similarity, was always observed. To test how well our model compares with experimental data, we present the cross-sectional area grain size distribution taken from data like that presented in Fig. 4 and compared with that measured for pure Fe in Fig. 6. Note that the grain size distribution function for the simulations and experiment agree remarkably well.

The mean grain size was also monitored as a function of time. In Fig. 7 we present the mean grain area for 2-d and the mean cross-sectional area for 3-d as a function of time. The growth kinetics for these two cases gave ($A \sim t^{2n}$) n = 0.41 ± 0.03 (2-d) (15) and n = 0.37 ± 0.02 (3-d) (23). For comparison, the average grain growth exponent n derived from averaging the results for n from the literature for different metals and ceramics is 0.39 ± 0.07 (11).

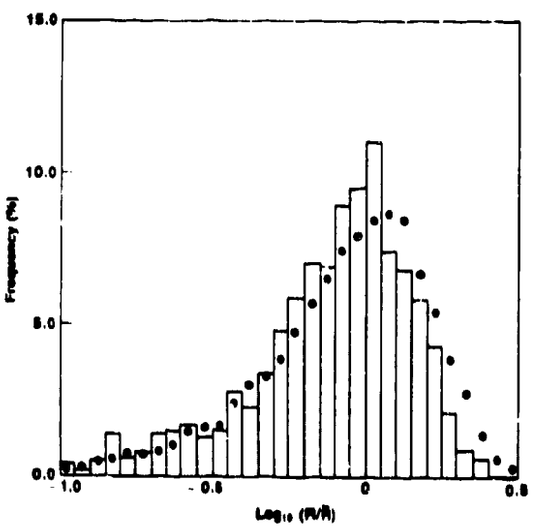

Figure 5 - Grain radius distribution as determined from cross-sections of the 3-d lattice model (filled circles) and from the 2-d lattice model (histogram).

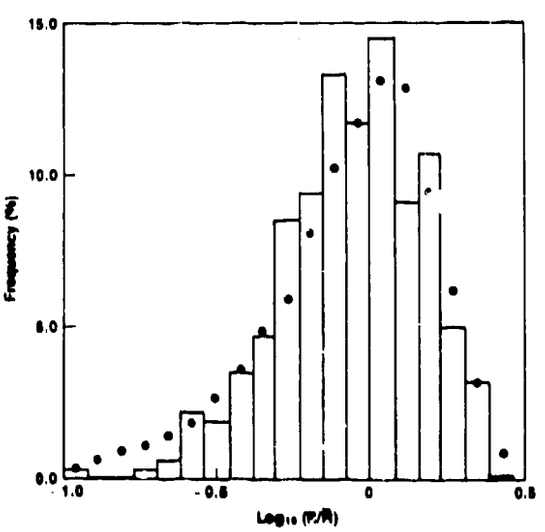

Figure 6 - Grain radius distribution as determined from a cross-sectional area analysis of pure Fe (histogram) and from cross-sections of the three-dimensional lattice model (filled circles).

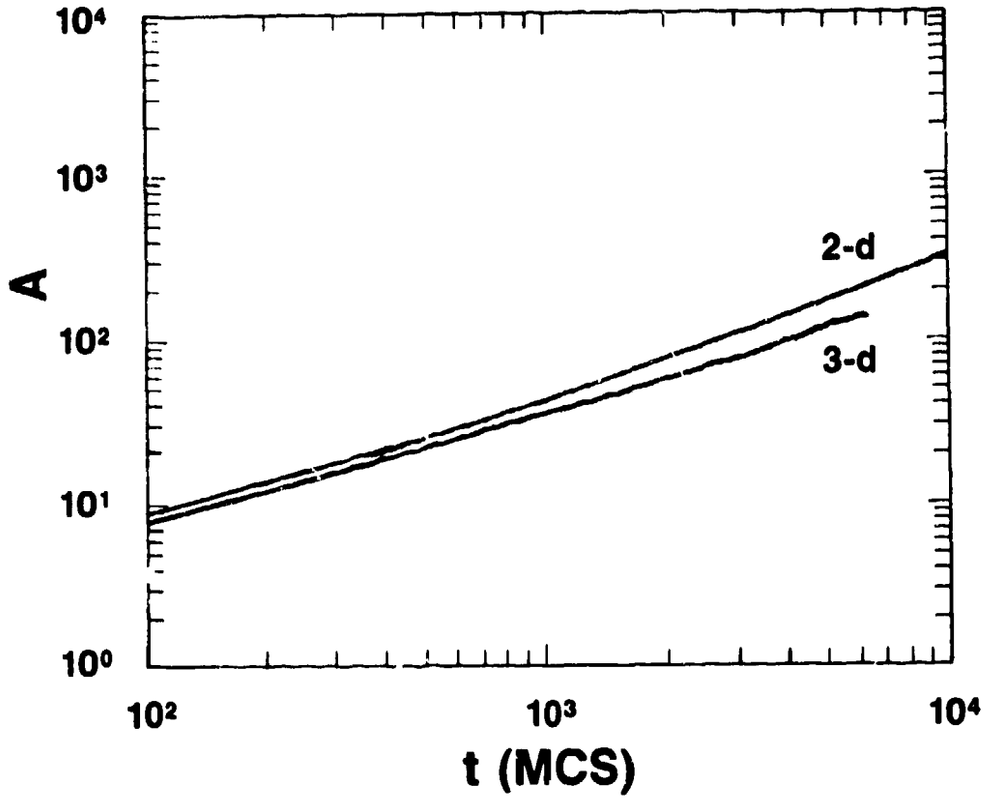

Figure 7 - Log-log plot of the mean area A versus time for Q = 48 for the two-dimensional grain growth simulations and for the cross-sectional data from the three-dimensional simulations.

One advantage of this method is that since grain topology is not averaged away, we can measure the topological distribution functions as shown in Fig. 8. Here we compare the results from our simulation in 3-d with those measured for Al (24), Sn (1), and MgO (25). In Fig. 9 we show the mean grain radius for each topological class versus the number of edges, N_e. In all cases, the agreement between the simulations of our lattice model and the experimental results is excellent.

One interesting question that often arises is why the growth exponent $n < 1/2$ in both our simulations and experiments. Recently, Mullins (22) has shown that by assuming statistical self-similarity (which our simulations demonstrate) and local equilibrium that n must equal 1/2 in 2-d. He uses the result, first proven by von Neumann (26) and Mullins (27), that for both bubble growth and idealized grain growth in 2-d, the rate of change of the area A_1 of an individual grain (or bubble) depends only on the number of sides,

$$A \equiv \frac{dA_1}{dt} = \frac{\pi k}{3}(N_e - 6) \qquad (3)$$

where k is a constant. This equation should be valid for an arbitrarily shaped two-dimensional grain of N_e-sides under the assumption that $u = k/R$ and the angle between intersecting grain boundaries is 120°. Here u is the local velocity and R is the signed local radius of curvature lying in the plane, counted positive when it lies along $\hat{n}$. Thus $A_1 > 0$ for $N_e > 6$ and is < 0 for $N_e < 6$. Writing the statistical self-similarity hypothesis in the form

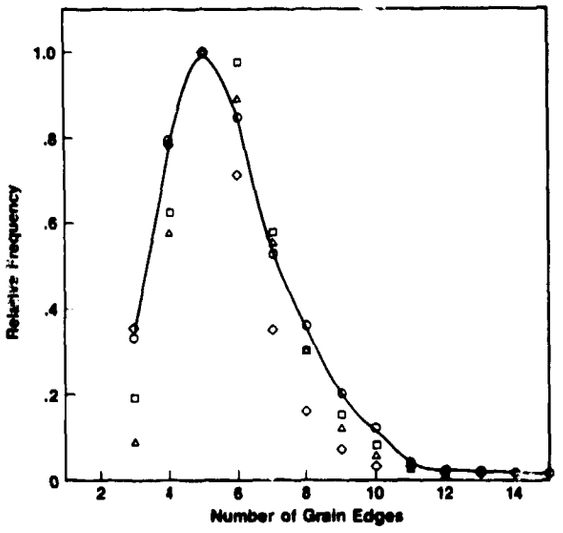

Figure 8 - Topological distribution for the number of grain edges measured in cross-section for the microstructure in Fig. 4 (circles), and for MgO (triangle), Al (squares), and Sn (diamond). The curve is drawn through the simulation results.

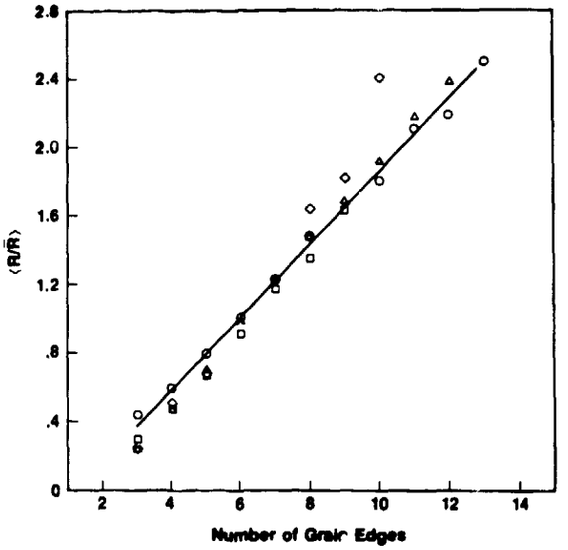

Figure 9 - Mean grain radius for each topological class versus number of edges N_e. The circles represent data from cross-section of the 3-d microstructures. The triangles and diamonds represent Aboav and Langdon's data on MgO (25), and Beck's data on Al (24), respectively. The squares represent the results obtained from the 2-d simulation. The line is drawn through the 3-d simulation results.

$$f_{N_e}(A,t) = \phi_{N_e}(A/\bar{A})/\bar{A} \qquad (4)$$

where $f_{N_e}(A,t)dA$ is the probability that a grain has N_e edges and area between $\bar{A}$ and $A + dA$, Mullins (22) then proves that if local equilibrium is satisfied [Eq. (3) is valid for all grains at all times] then $n = 1/2$.

Since we have already shown (16) that Eq. (4) is valid, it is of interest to test Eq. (3). We first performed a grain growth simulation in 2-d for 1,000 MCS until there were 960 grains remaining. We then followed each grain, monitoring its number of edges as a function of time. In Fig. 10, we present results for the temporal evolution of the area of several individual grains with the same number of edges. Those grains monitored in Fig. 10 were highly unusual in that their number of edges did not change during the majority of the 10,000 MCS step run. For convenience we have reset the clock to 0 after we started monitoring the number of edges and we have plotted a symbol only when the number of edges equal the number N_e specified in the figure. In Fig. 4, we have shaded those grains which remain predominantly 6 edged during the 10,000 MCS run. From Fig. 10, we see that the slope of A_i is approximately zero for $N_e = 6$ and that for $N_e = 4$ is approximately of equal magnitude and opposite sign from that for $N_e = 8$. An average slope for $N_e = 5$ and 7 is harder to determine. We also must point out, however, that most of the grains change N_e too often to be plotted in this way. Shown in Fig. 11 is the temporal evolution of the area, A_i, for five more typical grains. A different symbol is used to

Thus it appears that for those grains which keep the same number of sides for a long time, Eq. (3) is satisfied. However, there are large fluctuations around the mean slope and for most grains Eq. (3) is not applicable. From these results, we can understand the discrepancy in the value of n between classical theories (1-5) and our simulations. Since local equilibrium, Eq. (3), is never established, the grain growth is slower than would be expected. The grains are continuously changing their number of edges N_e too rapidly for the system to reach local equilibrium.

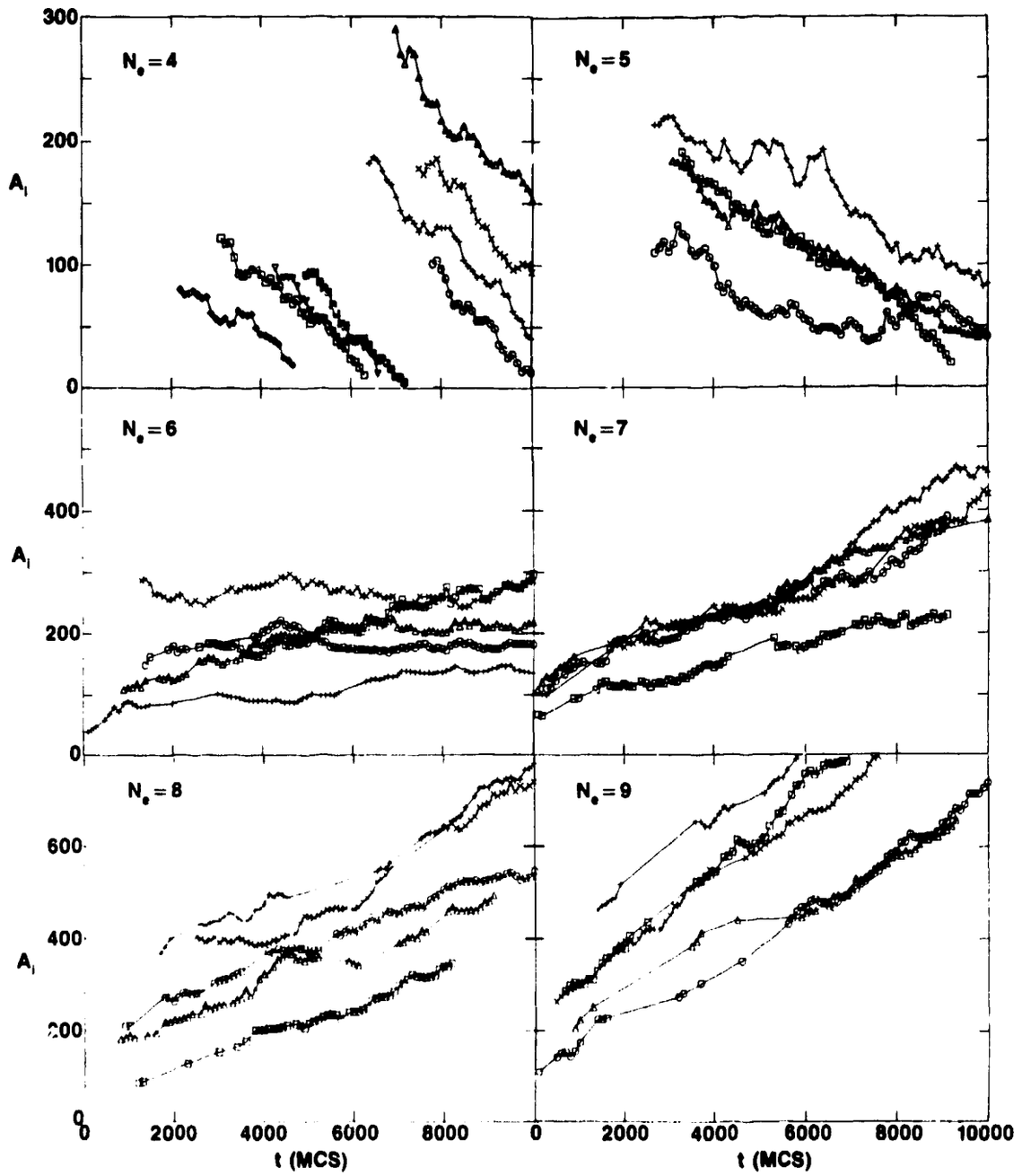

Figure 10 - Time dependence of the area, A_i, of individual grains from the 2-d simulations with a specific number of edges, N_e. Symbols are shown every 20 MCS when the grain has the number of edges specified. The simulation was started from a random starting state and run for 1,000 MCS, after which the clock was reset to 0. The data plotted are for grains which had the specified number of edges over unusually large portions of the 10,000 MCS simulation.

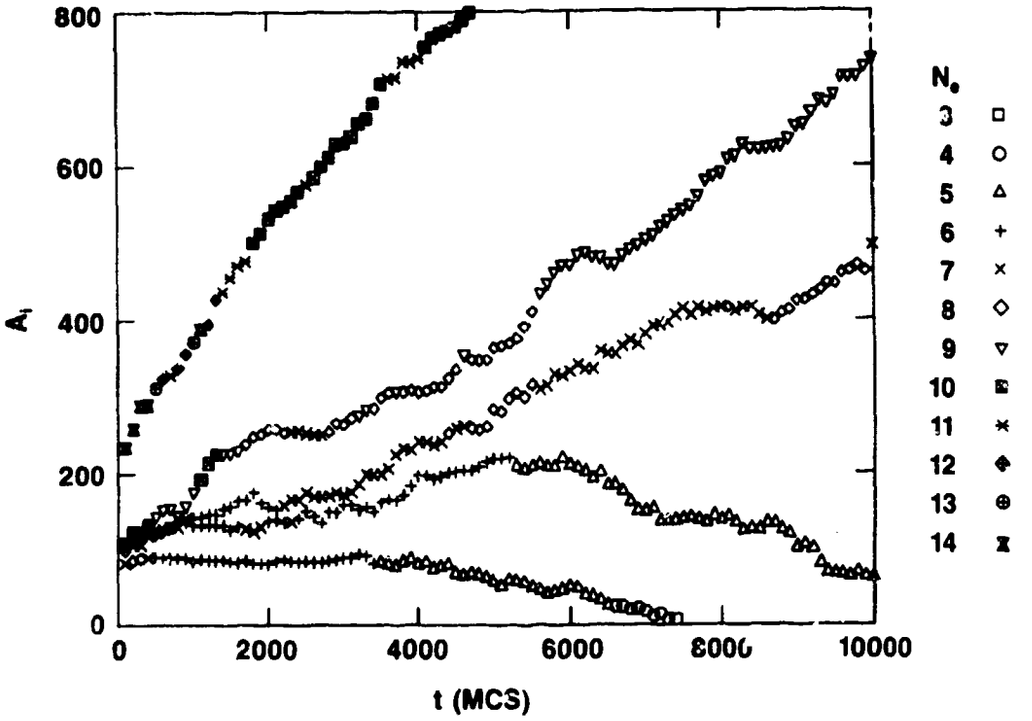

Figure 11 - Time dependence of the area A_i of five randomly chosen grains from the 2-d simulations. The symbols represent the number of edges, N_e. As in Fig. 10, the clock was reset to 0 after an initial run of 1,000 MCS.

Every time N_e changes, the microstructure rearranges to accomodate the new growth rate, as per Eq. (3). This accomodation process is not instantaneous but requires a finite amount of time, τ, which scales with the grain size. Since grain topology changes so frequently, it is likely that local equilibrium is never established and Eq. (3) is only rarely satisfied. This point of view is further supported by simulations of Weaire et al. for 2-d soap bubbles (28). Using a procedure similar to ours, they (29) introduced the additional constraint that Eq. (3) be satisfied locally at all times. The growth kinetics then followed Eq. (1) with $n = 1/2$. Without imposing Eq. (3), they obtained the same value of n as we found. It is important to note that statistical self-similarity requires only that $R \sim t^n$, not that $n = 1/2$!

Discussion

Now that we have demonstrated that our lattice models produce many of the essential features of grain growth in simple, isotropic system, it is possible to study more complex situations. In the presence of a particle dispersion (30), the average grain size R grows algebraically in time according to Eq. (1), with $n \sim 0.40$ (2-d), followed by a transition to a pinned state. There does, however, exist a cross-over regime where some grains have already becomed pinned and hence the kinetics are not adequately described by Eq. (1). The final average grain area and the time required for the microstructure to pin are both approximately proportional to the inverse particle concentration in 2-d. In the presence of anisotropic grain boundary energies (31), the growth exponent n is found to decrease in 2-d from $n = 0.42 \pm 0.02$ to 0.25 ± 0.02 and the grain size distribution broadens, as the anisotropy is increased. However, for values of the anisotropy expected for real polycrystalline materials, the results differ only slightly from those measured in the isotropic case. In

been studied. Results from this work will be presented in these proceedings (20).

We think that we have demonstrated that although the lattice model employed in the simulation described above is inherently discrete, the resultant micrographs show an excellent correspondence with those from real materials. The constraints imposed upon the boundary intersections due to the symmetry of the underlying lattice appears to be unimportant, and the interface tension dictates the angle at which grain boundaries meet. What is somewhat surprising is the agreement between the two-dimensional results and the cross-sections of the three-dimensional systems. While the grain radii distribution function as computed from the volume is narrower than the grain radii taken from the cross-sectional area, the grain radii taken from the cross-sectional area in 3-d are nearly identical to those found in the 2-d simulations.

One further test of the validity of the lattice model is the comparison of kinetic predictions with experiment. Kinetics measured from the mean chord, area and volume give the same growth exponent, n, in 3-d. While we do not know if the difference in n between 2-d and 3-d is significant, both results agree very well with experimental findings and disagree with existing grain growth theories (n=1/2). While one cannot rule out that asymptotically both the simulations and experiments would not eventually cross over to n = 1/2, we see no physical reason why the growth of a grain in an average environment should be the same as that occurring in the presence of many, competing grains. In addition, the fact that both the kinetics and all of the measured grain size distributions agree so well with experiment, suggests that the model has captured the essential features of the grain growth, at least on the time scale of an experimentalist.

REFERENCES

1. P. Feltham, Acta Metall. 5, 97 (1957).
2. F. N. Rhines and K. R. Craig, Met. Trans. 5, 413 (1974).
3. M. Hillert, Acta Metall. 13, 227 (1965).
4. N. P. Louat, Acta Metall. 22, 721 (1974).
5. S. K. Kurtz and F. M. A. Carpay, J. Appl. Phys. 51, 5725 (1981).
6. R. D. Cook, Concepts and Applications of Finite Element Analysis, Wiley, New York (1974).
7. J. Kushick and B. J. Berne, in Statistical Mechanics B; Time Dependent Processes (editor B. J. Berne) Plenum, New York (1977), p. 41.
8. W. L. Bragg and J. F. Nye, Proc. Royal Soc. A190, 474 (1977).
9. J. L. Finney, Ph.D. Thesis, University of London, 1958.
10. J. W. Dally and W. F. Riley, Experimental Stress Analysis, McGraw-Hill, New York (1978).
11. F. Haessner, Recrystallization of Metallic Materials, edited by F. Haessner, Riederer-Verlay, Stuttgart (1978), p. 63.
12. O. Hunderi, N. Ryum and H. Westengen, Acta Metall. 27, 161 (1979); 29, 1737 (1981).
13. V. Yu Novikov, Acta Metall. 26, 1739 (1978); 27, 1461, (1979).
14. D. J. Srolovitz, M. P. Anderson, G. S. Grest and P. S. Sahni, Scripta Metall. 17, 241 (1983).
15. M. P. Anderson, D. J. Srolovitz, G. S. Grest and P. S. Sahni, Acta Metall. 32, 783 (1984).
16. D. J. Srolovitz, M. P. Anderson, P. S. Sahni and G. S. Grest, Acta Metall. 32, 793 (1984).
17. P. S. Sahni, D. J. Srolovitz, G. S. Grest, M. P. Anderson and S. A.

18. M. J. Buerger, X-Ray Crystallography, Wiley, New York (1942).
19. J. A. Venables, Developments in Electron Microscopy and Analysis, Academic Press, New York (1976).
20. M. P. Anderson, G. S. Grest and D. J. Srolovitz, This Proceedings
21. G. S. Grest, S. A. Safran and P. S. Sahni, J. Appl. Phys. 55, 2432 (1984).
22. W. W. Mullins (to be published).
23. M. P. Anderson, G. S. Grest, and D. J. Srolovitz, Scripta Metall. 19, 225 (1985).
24. P. A. Beck, Phil. Mag., Suppl. 3, 245 (1954).
25. D. A. Aboav and T. G. Langdon, Metallography 1, 333 (1969).
26. J. von Neumann, in Metal Interfaces, p. 108, ASM, Metals Park, Ohio (1952).
27. W. W. Mullins, J. Appl. Phys. 27, 900 (1956).
28. D. Weaire and J. P. Kermode, Phil Mag. 50, 379 (1984).
29. D. Weaire, private communication.
30. D. J. Srolovitz, M. P. Anderson, G. S. Grest and P. S. Sahni, Acta. Metall. 32, 1429 (1984).
31. G. S. Grest, M. P. Anderson and D. J. Srolovitz, Acta Metall. 33, 509 (1985).
32. D. J. Srolovitz, G. S. Grest and M. P. Anderson, Acta Metall., in press.
33. D. J. Srolovitz, G. S. Grest and M. P. Anderson, submitted to Acta Metall.